Evidence for Kosterlitz-Thouless and three-dimensional *XY* critical behavior in $Bi_2Sr_2CaCu_2O_{8+\delta}$

S. Weyeneth* and T. Schneider
Physik-Institut der Universität Zürich, Winterthurerstrasse 190, CH-8057 Zürich, Switzerland

E. Giannini
DPMC, University of Geneva, 24 Quai Ernest-Ansermet, CH-1211 Geneva 4, Switzerland
(Received 6 February 2009; revised manuscript received 17 April 2009; published 4 June 2009)

We present reversible magnetization data of a high-quality $Bi_2Sr_2CaCu_2O_{8+\delta}$ single crystal and explore the occurrence of three-dimensional (3D)-*xy* critical behavior close to the bulk-transition temperature T_c and of Kosterlitz-Thouless (KT) behavior. Below and above the presumed Kosterlitz-Thouless transition temperature T_{KT} we observe the characteristic two-dimensional (2D)-*xy* behavior: a downward shift in the crossing point phenomenon toward T_{KT} as the field is decreased and sufficiently below T_{KT} the characteristic 2D-*xy* relationship between the magnetization and the in-plane magnetic penetration depth λ_{ab}. In contrast, the measured temperature dependence of the superfluid density does not exhibit the characteristic KT behavior around the presumed T_{KT}. The absence of this feature is traced back to the 2D- to 3D-*xy* crossover setting in around and above T_{KT}. Invoking the Maxwell relation, the anomalous field dependence of the specific-heat peak is also traced back to the intermediate 2D-*xy* behavior. However, close to T_c we observe consistency with 3D-*xy* critical behavior in agreement with measurements of λ_{ab}.

DOI: 10.1103/PhysRevB.79.214504 PACS number(s): 74.72.−h, 74.25.Bt, 74.25.Dw

I. INTRODUCTION

The study of thermal fluctuations received a considerable impetus from the discovery of the cuprate superconductors.[1–6] It was realized that in these materials the critical regime where thermal fluctuations dominate can be attained and that some of them are in addition quasi-two-dimensional (2D).[7] Furthermore, the systematics of the superconducting properties uncovered that the anisotropy is further enhanced with underdoping.[2,7] In this quasi-2D limit one expects the thermodynamic properties to be close to those of a two-dimensional superconductor, or more precisely of a stack of decoupled two-dimensional superconducting sheets. Although approximate treatments have been invoked to describe the thermodynamic properties of such materials, the essential ingredient, the Kosterlitz-Thouless (KT) behavior of the associated zero-field transition,[8] has mostly not been taken into account.[9–11] Only recently, this behavior was incorporated by combining Kosterlitz-Thouless renormalization group flows and explicit computations for plasmas.[12] On this basis the field and temperature dependences of the magnetization density, $m(H_c,T)$, for temperatures T near to and below the KT transition temperature T_{KT} were determined for magnetic fields H_c applied perpendicular to the superconducting sheet. These results are interesting on three immediate fronts. First, the resulting trends in the magnetization appear to emerge from the recent $Bi_2Sr_2CaCu_2O_{8+\delta}$ data of Li *et al.*[13] for underdoped and optimally doped samples. Second, by contrast evidence for smeared three-dimensional (3D)-*xy* behavior stems from the measured temperature dependence of the in-plane magnetic penetration depth λ_{ab}.[14–17] Third, the magnetic field dependence of the specific-heat peak exhibits, opposite to the generic behavior,[4,6] a shift to higher temperatures with increasing field strength.[18]

In this study we present reversible magnetization data of a $Bi_2Sr_2CaCu_2O_{8+\delta}$ single crystal and explore the evidence for intermediate KT-(2D-*xy*) and 3D-*xy* critical behavior. Below $T=89.5$ K $\simeq T_{KT}$ we observe consistency with the KT behavior in terms of the characteristic $m\propto\ln(H_c)$ dependence at fixed temperature. Furthermore, invoking the Maxwell relation $\partial^2 M/\partial T^2|_{H_c}=\partial(C/T)/\partial H_c|_T$ the anomalous field dependence of the specific heat peak is also traced back to 2D-*xy* behavior. However, close to the bulk-transition temperature $T_c\simeq 91.21$ K we observe consistency with 3D-*xy* critical behavior, consistent with previous measurements of the in-plane magnetic penetration depth λ_{ab}.[14,16,17] In Sec. II we sketch the theoretical background including the scaling relations for 2D- and 3D-*xy* critical behavior. Section III is devoted to the experimental details, and in Sec. IV we present the analysis of the data uncovering the evidence for 2D-*xy* and 3D-*xy* critical behavior in the respective temperature regimes. We close with a brief summary and some discussion.

II. THEORETICAL BACKGROUND

When thermal fluctuations dominate and the coupling to the charge is negligible a bulk superconductor is expected to exhibit sufficiently close to T_c 3D-*xy* critical behavior. In this case the magnetization per unit volume, $m=M/V$, adopts the scaling form[2–6,19]

$$\frac{m}{TH_c^{1/2}}=-\frac{Q^{\pm}k_B\xi_{ab}}{\Phi_0^{3/2}\xi_c}F^{\pm}(z),\quad F^{\pm}(z)=z^{-1/2}\frac{dG^{\pm}}{dz},$$

$$z=x^{-1/2\nu}=\frac{(\xi_{ab0}^{\pm})^2|t|^{-2\nu}H_c}{\Phi_0}. \tag{1}$$

In this form $Q^{\pm}$ is a universal constant and $G^{\pm}(z)$ is a universal scaling function of its argument, with $G^{\pm}(z=0)=1$. In addition $\gamma=\xi_{ab}/\xi_c$ denotes the anisotropy, ξ_{ab} the zero-field in-plane correlation length, and H_c the magnetic field applied along the c axis. In terms of the variable x the scaling form

[Eq. (1)] is similar to Prange's result for Gaussian fluctuations.[20] Approaching T_c the correlation lengths diverges as

$$\xi_{ab,c} = \xi^{\pm}_{ab0,c0}|t|^{-\nu}, \quad t = T/T_c - 1, \quad \pm = \mathrm{sgn}(t). \tag{2}$$

Supposing that 3D-xy fluctuations dominate the critical exponents are given by[21]

$$\nu \simeq 0.671 \simeq 2/3, \quad \alpha = 2 - 3\nu \simeq -0.013, \tag{3}$$

and there are the universal critical amplitude relations[2–4,19,21]

$$\frac{\xi^{-}_{ab0}}{\xi^{+}_{ab0}} = \frac{\xi^{-}_{c0}}{\xi^{+}_{c0}} \simeq 2.21, \quad \frac{Q^{-}}{Q^{+}} \simeq 11.5, \quad \frac{A^{+}}{A^{-}} = 1.07, \tag{4}$$

and

$$A^{-}\xi^{-}_{a0}\xi^{-}_{b0}\xi^{-}_{c0} \simeq A^{-}(\xi^{-}_{ab0})^2\xi^{-}_{c0} = \frac{A^{-}(\xi^{-}_{ab0})^3}{\gamma} = (R^{-})^3,$$

$$R^{-} \simeq 0.815, \tag{5}$$

where $A^{\pm}$ is the critical amplitude of the specific-heat singularity, defined as

$$c = \frac{C}{Vk_B} = \frac{A^{\pm}}{\alpha}|t|^{-\alpha} + B, \tag{6}$$

where B denotes the background. The anisotropy is then characterized in terms of

$$\gamma = \frac{\xi_{ab}}{\xi_c} = \frac{\xi^{\pm}_{ab0}}{\xi^{\pm}_{c0}}. \tag{7}$$

Furthermore, in the 3D-xy universality class T_c, ξ^{-}_{c0} and the critical amplitude of the in-plane magnetic penetration depth λ_{ab0} are not independent but are related by the universal relation,[2–4,19]

$$k_B T_c = \frac{\Phi_0^2}{16\pi^3}\frac{\xi^{-}_{c0}}{\lambda^2_{ab0}} = \frac{\Phi_0^2}{16\pi^3}\frac{\xi^{-}_{ab0}}{\gamma\lambda^2_{ab0}}. \tag{8}$$

The existence of the magnetization at T_c of the magnetic penetration depth below T_c and of the magnetic susceptibility above T_c implies the following asymptotic forms of the scaling function,[2–4,19]

$$Q^{\pm}\frac{1}{\sqrt{z}}\left.\frac{dG^{\pm}}{dz}\right|_{z\to\infty} = Q^{\pm}c^{\pm}_{\infty},$$

$$Q^{-}\left.\frac{dG^{-}}{dz}\right|_{z\to 0} = Q^{-}c^{-}_{0}(\ln z + c_1),$$

$$Q^{+}\frac{1}{z}\left.\frac{dG^{+}}{dz}\right|_{z\to 0} = Q^{+}c^{+}_{0}, \tag{9}$$

with the universal coefficients

$$Q^{-}c^{-}_{0} \simeq -0.7, \quad Q^{+}c^{+}_{0} \simeq 0.9, \quad Q^{\pm}c^{\pm}_{\infty} \simeq 0.5, \quad c_1 \simeq 1.76. \tag{10}$$

Noting that $Bi_2Sr_2CaCu_2O_{8+\delta}$ is highly anisotropic ($\gamma \gg 1$),[22] the system is expected to exhibit away from T_c 2D-xy behavior. A characteristic property of 2D-superconductors emerges from the magnetic field dependence of the magnetization. Sufficiently below the Kosterlitz-Thouless transition temperature T_{KT} the magnetization is given by[12]

$$m = -\frac{\pi\rho_s(T)}{2d\Phi_0}\left(1 - \frac{k_B T}{\pi\rho_s(T)}\right)\ln\left(\frac{\Phi_0}{4\pi H_c a_0^2\gamma_3}\right)$$

$$= -\left(\frac{\Phi_0}{32\pi^2\lambda^2_{ab}(T)} - \frac{k_B T}{d\Phi_0}\right)\ln\left(\frac{\Phi_0}{4\pi H_c a_0^2\gamma_3}\right), \tag{11}$$

where ρ_s is the 2D superfluid density, related to the in-plane magnetic penetration depth λ_{ab} via

$$\rho_s(T) = \frac{d\Phi_0^2}{16\pi^3\lambda^2_{ab}(T)}. \tag{12}$$

Here d is the thickness of the independent superconducting sheets, γ_3 is a parameter that vanishes as T approaches T_{KT}, and a_0 is the microscopic short-distance cutoff length. Moreover, $\rho_s(T_{KT})$ and T_{KT} are related by

$$\rho_s(T_{KT}) = \frac{2}{\pi}k_B T_{KT}, \tag{13}$$

while $\rho_s(T)=0$ above T_{KT}. Below this universal Nelson-Kosterlitz jump $1/\lambda^2_{ab}(T)$ increases as[23,24]

$$\lambda^2_{ab}(T_{KT})/\lambda^2_{ab}(T) = \frac{T}{T_{KT}}[1 + \hat{b}(T_{KT} - T)^{1/2}]. \tag{14}$$

Note that Eq. (11) gives a simple relation between the superfluid density and the derivative of the magnetization, namely,

$$\frac{dm}{d\ln(H_c)} = g(T) = \frac{\Phi_0}{32\pi^2\lambda^2_{ab}(T)} - \frac{k_B T}{d\Phi_0}. \tag{15}$$

Furthermore, at criticality m depends on H in terms of[12]

$$m = -\frac{k_B T_{KT}}{d\Phi_0}\ln\left(\gamma_1 \ln\frac{\Phi_0}{4\pi H_c a_0^2\gamma_2}\right), \tag{16}$$

where γ_1 and γ_2 are constants. Correspondingly, plots of M vs T at different fields should then exhibit a systematic drift of the "crossing phenomenon." Above T_{KT} and for asymptotically small fields the magnetization is given by[12,30,31]

$$m \simeq -\frac{k_B T}{2d\Phi_0^2}\xi^2_{ab}H_c, \quad \xi_{ab} = \xi_{ab0}\exp\left(\frac{\tilde{b}}{(T/T_{KT} - 1)^{1/2}}\right), \tag{17}$$

where ξ_{ab} is the Kosterlitz-Thouless correlation length.[8] The parameters $\tilde{b}$ and $\hat{b}$, determining the temperature dependence of the magnetic penetration depth below the jump [Eq. (14)], are related by[24]

$$\tilde{b}\hat{b} = \pi/(2T_{KT}^{1/2}) \simeq 0.17 \ \mathrm{K}^{-1/2}. \tag{18}$$

III. EXPERIMENTAL DETAILS

Single crystals of $Bi_2Sr_2CaCu_2O_{8+\delta}$ were grown with the floating zone (FZ) method, from direct crystallization from

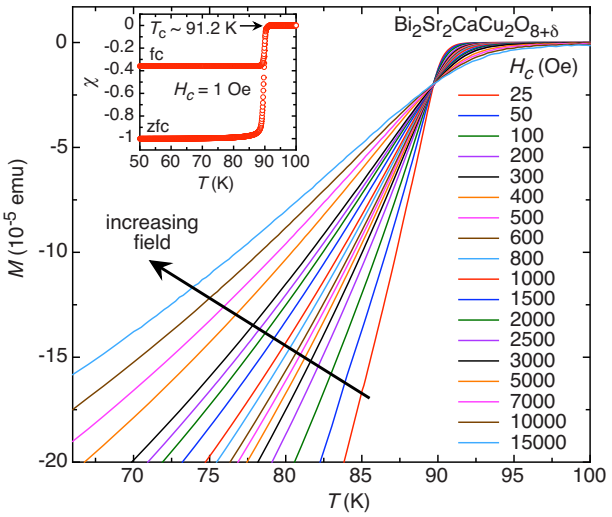

FIG. 1. (Color online) Temperature dependence of the measured reversible magnetic moment of the studied $Bi_2Sr_2CaCu_2O_{8+\delta}$ single crystal at various magnetic fields applied along the c axis. The inset depicts susceptibility measurements in 1 Oe in the ZFC and FC mode. The sharp onset of superconductivity points to a transition temperature close to $T_c \simeq 91.2$ K.

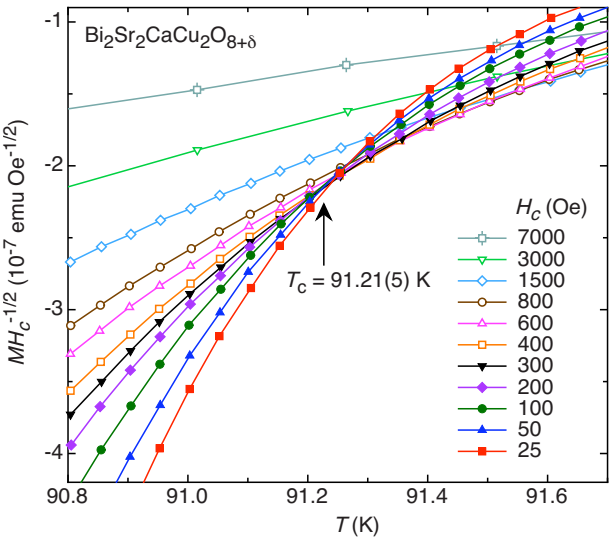

FIG. 2. (Color online) $M/H_c^{1/2}$ vs T yielding the estimate $T_c \simeq 91.21$ K in terms of the crossing point at $M/H_c^{1/2} \simeq -2.13 \times 10^{-7}$ emuOe$^{-1/2}$.

the melt (no solvent used). The feed rod was obtained from a commercial $Bi_2Sr_2CaCu_2O_{8+\delta}$ powder after pressing and sintering to a shape of 7 cm in length and about 7 mm in diameter. The seed rod was made with a previously crystallized rod. After a first fast FZ melting at a rate of 24 mm/h in Ar, the crystal growth was performed at a slow rate of 0.2 mm/h in a 7% O_2–93% Ar atmosphere, while both rods were counter-rotating at 18 rpm. The FZ growth was performed in a commercial two-mirror vertical furnace (from Cyberstar), equipped with two 1000 W halogen lamps. The growth conditions at the flat zone interface were kept stable for several days. A review of the growth technique can be found elsewhere.[25] The as-grown crystals were easily cleaved from the crystallized boule and annealed at $T = 500$ °C for 50 h in 0.1% O_2–99.9% Ar in order to tune and homogenize the oxygen content corresponding to the optimal doping level. Crystals with typical size of 1–5 mm and thickness of 0.05–0.1 mm could be extracted. The good crystalline quality of the samples was checked by x-ray diffraction and magnetic susceptibility measurements.

The $Bi_2Sr_2CaCu_2O_{8+\delta}$ sample used in this work, a $V \simeq 4.6 \times 10^{-5}$ cm^3 single crystal, was chosen by its sharp low-field Meissner transition from several high-quality single crystals. The magnetization was measured in a magnetic property measurement system (MPMS) XL from Quantum Design, equipped with a reciprocating sample option. The inset in Fig. 1 shows the measured susceptibility at $H_c = 1$ Oe applied along the c axis. It reveals a rather sharp transition at $T_c \simeq 91.2$ K and a well-saturated Meissner state, pointing to excellent quality. The volume of the sample was estimated by susceptibility measurements below T_c in the Meissner state with a magnetic field applied along the ab plane to minimize demagnetization effects. The extracted volume of $V \simeq 4.6 \times 10^{-5}$ cm^3 compares well with that estimated with an optical microscope. Figure 1 summarizes the measured temperature dependence of the magnetic moment at fields ranging from 25–15 000 Oe applied along the c axis. After applying the magnetic field, well below T_c it was kept constant and the magnetic moment of the single crystal was measured at a stabilized temperature by moving the sample with a frequency of 0.5 Hz through a set of detection coils. The reversible superconducting diamagnetic magnetization, $M = mV$, was then obtained by comparing field-cooled (FC) and zero-field-cooled (ZFC) data. Due to a substantial pinning contribution at low magnetic field we omitted data below 25 Oe. A temperature-dependent normal-state paramagnetic background was subtracted.

IV. DATA ANALYSIS

We are now prepared to analyze the magnetization data. To estimate the bulk T_c we invoke Eqs. (1), (9), and (10), revealing that the plot $m/H_c^{1/2}$ vs T should exhibit a crossing point at T_c. Here $m/(TH_c^{1/2})$ adopts with Eq. (7) the value $m/(T_c H_c^{1/2}) = -0.5 k_B \gamma \Phi_0^{-3/2}$. According to Fig. 2, showing $M/H_c^{1/2}$ vs T there is a crossing point at $T_c \simeq 91.21$ K where $M/H_c^{1/2} \simeq -2.13 \times 10^{-7}$ emuOe$^{-1/2}$. With $V \simeq 4.6 \times 10^{-5}$ cm^3, where $m = M/V$, it yields for the anisotropy [Eq. (7)] the estimate,

$$\gamma = \bar{\xi}_{ab0}/\bar{\xi}_{c0} \simeq 69, \tag{19}$$

compared to $\gamma \simeq 133$ for an underdoped sample with $T_c \simeq 84.2$ K and in reasonable agreement with earlier estimates for optimally doped samples.[22,26] Given this rather large anisotropy the 2D- to 3D-xy crossover is expected to occur rather close to the bulk T_c.

A characteristic feature of a 2D superconductor is the crossing phenomenon occurring at fixed magnetic fields and above T_{KT} in the plot M vs T.[2,12] A glance at Fig. 3 reveals that this phenomenon is well confirmed above $T = 89.5$ K $\simeq T_{KT}$. Indeed, there is as predicted a downward shift in the

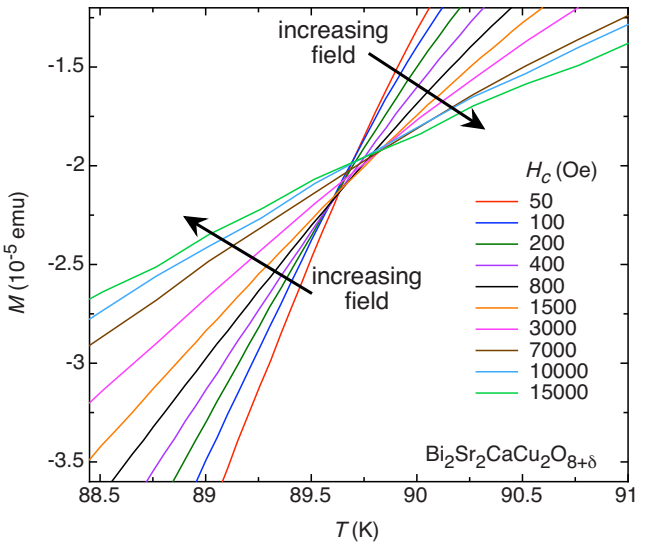

FIG. 3. (Color online) M vs T at various magnetic fields exhibiting a crossing phenomenon shifting toward $T_{KT} \simeq 89.5$ K from above as the field is decreased.

"crossing point" toward T_{KT} from above as the field is decreased.[12] The same behavior was also observed in the highly anisotropic Tl-1223, Bi-2201, and underdoped $La_{2-x}Sr_xCuO_4$ single crystals.[2,27–29]

To substantiate 2D-xy behavior further we invoke Eq. (11) in terms of the plot M vs H_c shown in Fig. 4. The solid lines in Fig. 4(a) indicate that sufficiently below $T_{KT} \simeq 89.5$ K the 2D relation [Eq. (15)] between the superfluid density and the derivative of the magnetization with respect to the logarithm of the field is for small fields well obeyed, so in this temperature regime the system indeed behaves as a stack of essentially decoupled two-dimensional Kosterlitz-Thouless films with $T_{KT} \simeq 89.5$ K. However, close to the bulk $T_c \simeq 91.21$ K one expects 3D-xy critical behavior. In this case and in the magnetic field range considered here the limit $z \rightarrow \infty$ is then approached. Here Eqs. (1), (9), and (10) imply the limiting behavior

$$m = -\frac{Q^+ c_\infty^+ k_B \xi_{ab} T}{\Phi_0^{3/2} \xi_c} H_c^{1/2} \simeq -\frac{0.5 k_B \xi_{ab0}^+ T}{2\Phi_0^{3/2} \xi_{c0}^+} H_c^{1/2}. \quad (20)$$

Figure 4(b), depicting M vs H_c close to $T_c \simeq 91.21$ K at $T=91$, 91.25, and 91.5 K, shows that this expectation is well confirmed. According to this, approaching T_c the system undergoes a 2D- to 3D-xy crossover. It implies that the characteristic 2D-xy critical behavior, including the jump of the superfluid density at T_{KT} [Eqs. (13) and (14)], is removed.

To clarify this point we invoke Eq. (11) to determine the temperature dependence of $1/\lambda_{ab}^2$ sufficiently below T_{KT}. Setting $M(H_c,T)=f(T)+g(T)\cdot\ln(H_c)$, $g(T)$ is then given by Eq. (15) and follows from plots as shown in Fig. 4(a) in terms of the slope of the straight lines. For $d=30$ Å we obtain for $1/\lambda_{ab}^2(T)$ the data points shown in Fig. 5. For comparison we included the ab-plane microwave surface impedance data of Lee *et al.*[15] for a high-quality $Bi_2Sr_2CaCu_2O_8$ single crystal, plotted in terms of the superfluid density, assuming $\lambda_{ab}(0)=1350$ Å. Sufficiently below

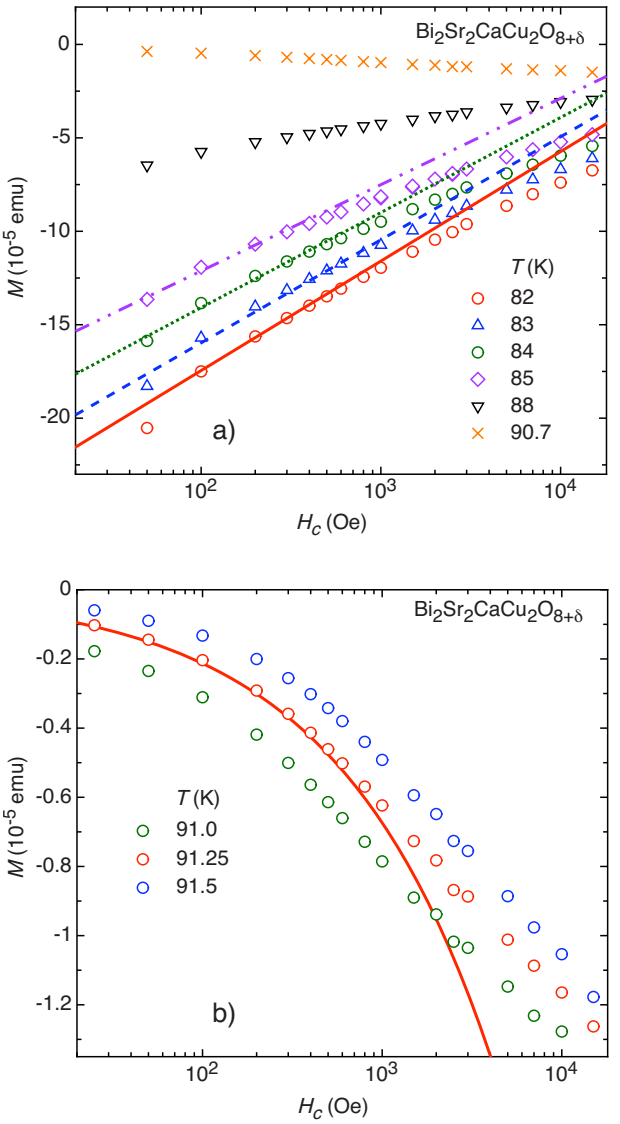

FIG. 4. (Color online) M vs H_c at various fixed temperatures. (a) From $T=82$ to 90.7 K. The straight lines indicate the characteristic 2D relation between the superfluid density and the derivative of the magnetization with respect to the logarithm of the field [Eq. (15)], valid in the low-field regime as long as pinning contributions are negligible. (b) M vs H_c at $T=91$, 91.25, and 91.5 K. The solid line is $M=-2.13\times10^{-7}\cdot H_c^{1/2}$ emu indicating the characteristic 3D-xy behavior at T_c in terms of Eq. (20).

T_{KT} we observe reasonable agreement with the 2D-xy prediction (●) and the measured $1/\lambda_{ab}^2(T)$ (■). Accordingly, in this regime the expulsion of vortices from the KT phase dominates. Here we also observe consistency with the characteristic KT behavior indicted by the dash-dot-dot line [Eq. (14)]. However, around T_{KT}, indicated by the horizontal and KT lines, the measured $1/\lambda_{ab}^2(T)$ does not exhibit any evidence for the characteristic jump from $1/\lambda_{ab}^2(T_{KT})$ to zero for $T>T_{KT}$. In contrast agreement with the leading 3D-xy critical behavior is observed (solid line), revealing the removal of the characteristic jump in $1/\lambda_{ab}^2(T)$ at T_{KT} due to the 2D- to 3D-xy crossover. To explore the effect of the 3D-xy fluctuations further, we use the critical amplitude, $1/\lambda_{ab0}^2=5$

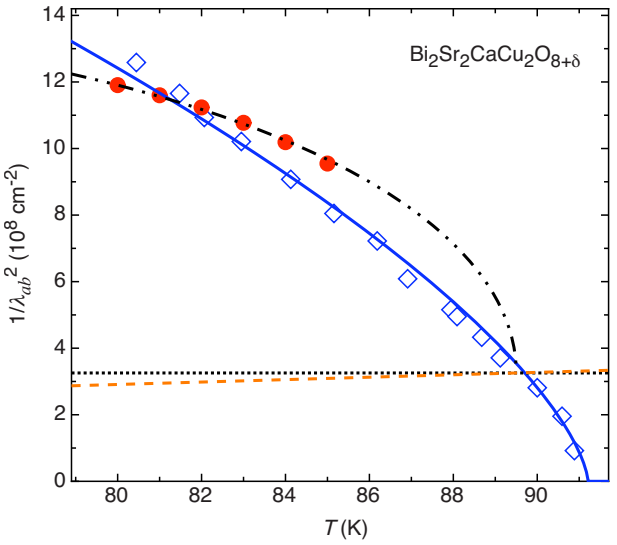

FIG. 5. (Color online) $1/\lambda_{ab}^2(T)$ vs T. ●: derived from the magnetization with the aid of Eq. (11) rewritten as $M(H_c,T)=f(T)+g(T)\cdot\ln(H_c)$ and $d=30$ Å; ■: experimental data derived from Lee *et al.* (Ref. 15) with $\lambda_{ab}(T=0)=1350$ Å. The solid line is $1/\lambda_{ab}^2(T)=1/\lambda_{ab0}^2(1-T/T_c)^{2/3}$ with $1/\lambda_{ab0}^2=5\times10^9$ cm^{-2} and $T_c=91.21$ K indicating 3D-xy critical behavior. The dashed line is the KT-line $1/\lambda_{ab}^2(T)=3.64\times10^6\cdot T$ cm^{-2} [Eq. (13)], the dotted one $1/\lambda_{ab}^2(T_{KT})=3.26\times10^8$ cm^{-2} with $T_{KT}=89.5$ K, and the dash-dot-dot one is Eq. (14) with $\hat{b}\simeq1$ K$^{-1/2}$.

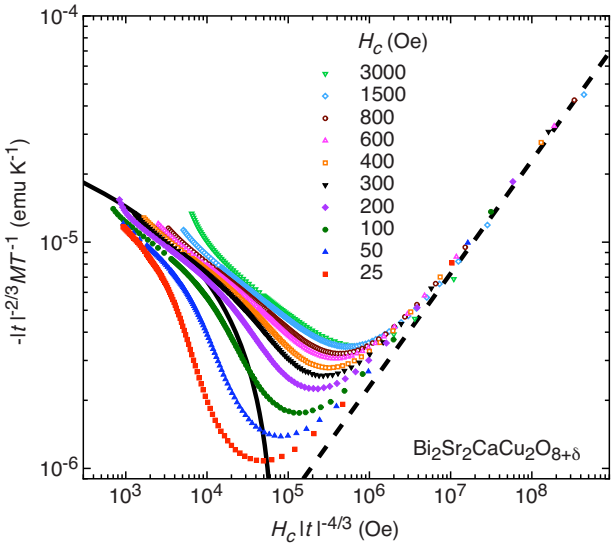

FIG. 6. (Color online) $-|t|^{-2/3}M/T$ vs $H_c|t|^{-4/3}$ for $T<T_c$ at various applied magnetic fields. The solid line is Eq. (25) and the dashed one Eq. (26).

$\times10^9$ cm^{-2} and $T_c=91.21$ K to obtain from the universal relation [Eq. (8)] the estimate

$$\bar{\xi}_{c0}\simeq 2.9 \text{ Å} \tag{21}$$

for the amplitude of the c-axis correlation length. The occurrence of 3D-xy critical behavior then requires that $\xi_c(T)=\bar{\xi}_{c0}|t|^{-2/3}$ exceeds d considerably, yielding with $d=30$ Å and $T_c=91.21$ K for the onset of 3D fluctuations the lower bound $T>90.24$ K. Furthermore, around and above $T=91$ K the 3D-xy critical regime is attained [see Fig. 4(b)]. So the occurrence of KT behavior in $1/\lambda_{ab}^2(T)$ is restricted to temperatures below $T_{KT}\simeq89.5$ K.

On the other hand, the small amplitude of the c-axis correlation length leads with $\gamma=69$ [Eq. (19)] to a rather large amplitude of the in-plane correlation length, $\bar{\xi}_{ab0}=\gamma\bar{\xi}_{c0}\simeq200$ Å and with the universal relation [Eq. (5)] to a very small amplitude of the specific-heat singularity,

$$A^-=\frac{0.815^3}{\gamma^2(\bar{\xi}_{c0})^3}\simeq4.7\times10^{-6} \text{ Å}^{-3}, \tag{22}$$

in comparison with $A^-\simeq6.8\times10^{-4}$ Å^{-3} in optimally doped $YBa_2Cu_3O_{7-\delta}$ and 1.7×10^{-3} Å^{-3} in ^{4}He.[2] This small critical amplitude renders it difficult to observe 3D-xy critical behavior in the specific heat of $Bi_2Sr_2CaCu_2O_{8+\delta}$.[18]

Considering Eqs. (1), (9), and (10) consistency with 3D-xy critical behavior also requires that the data scale below T_c as

$$|t|^{-2/3}\frac{m}{T}=-\frac{Q^-\bar{c}_0^-k_B}{\Phi_0\bar{\xi}_{c0}}\left[\ln\left(\frac{(\bar{\xi}_{ab0})^2}{\Phi_0}H_c|t|^{-4/3}\right)+c_1\right],\quad z\to0, \tag{23}$$

and

$$|t|^{-2/3}\frac{m}{T}=-\frac{Q^-\bar{c}_\infty^-k_B\bar{\xi}_{ab0}}{\Phi_0^{3/2}\bar{\xi}_{c0}}(H_c|t|^{-4/3})^{1/2},\quad z\to\infty, \tag{24}$$

respectively. In Fig. 6 we plot $-|t|^{-2/3}M/T$ vs $H_c|t|^{-4/3}$ for $T<T_c$ at various applied magnetic fields. The solid line is Eq. (23) in terms of

$$-|t|^{-2/3}\frac{M}{T}=-3.32\times10^{-6}[\ln(H_c|t|^{-4/3})-11.23] \text{ (emuK}^{-1}), \tag{25}$$

and the dashed one

$$-|t|^{-2/3}\frac{M}{T}=2.3\times10^{-9}(H_c|t|^{-4/3})^{1/2} \text{ (emuK}^{-1}) \tag{26}$$

corresponds to the limit [Eq. (24)]. While the $H_c|t|^{-4/3}\propto z\to\infty$ limiting behavior (dashed curve) is well confirmed we observe with decreasing z substantial deviations from the data collapse on a single curve.

From Eq. (26) we derive with $V=4.6\times10^{-5}$ cm^3, where $m=M/V$, the estimate

$$\gamma=\bar{\xi}_{ab0}/\bar{\xi}_{c0}\simeq68, \tag{27}$$

in reasonable agreement with $\gamma=\bar{\xi}_{ab0}/\bar{\xi}_{c0}\simeq69$ [Eq. (19)], derived from the crossing point in $M/H_c^{1/2}$ vs T shown in Fig. 2. The apparent failure of 3D-xy scaling outside the limit $H_c|t|^{-4/3}\propto z\to\infty$ is then attributable to the 3D- to 2D-xy crossover. In particular, very small magnetic fields would be required to attain the limit $H_c|t|^{-4/3}\propto z\to0$ with reduced temperatures t in the range where 3D-xy fluctuations dominate.

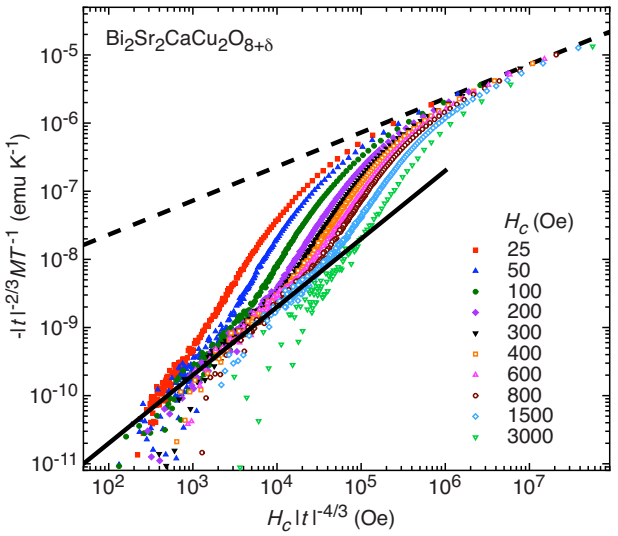

FIG. 7. (Color online) $-|t|^{-2/3}M/T$ vs $H_c|t|^{-4/3}$ for $T>T_c$ at various applied magnetic fields. The solid line is Eq. (30) and the dashed one Eq. (31).

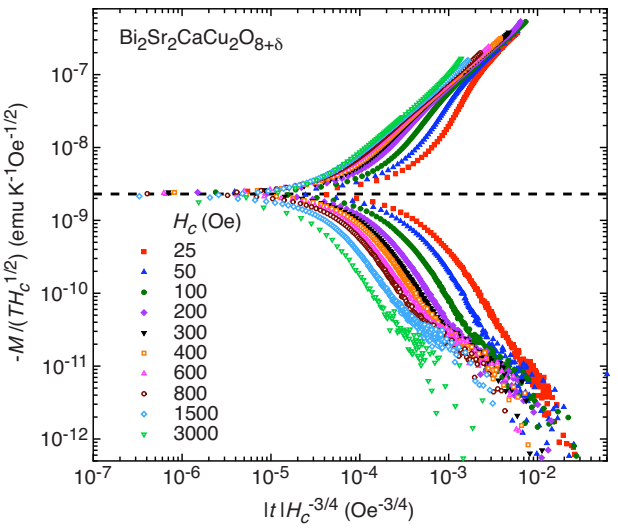

FIG. 8. (Color online) $-M/(TH_c^{1/2})$ vs $|t|H_c^{-3/4}$ at various applied magnetic fields. The dashed line is Eq. (31).

Indeed, given our evidence for 2D-xy behavior above $T_{KT} \simeq 89.5$ K in terms of the crossing phenomenon (Fig. 3) and 3D-xy critical behavior above $T=91$ K [Fig. 4(b)], transforming to $H_c|t|^{-4/3}=2\times10^6$ Oe for $H_c=600$ Oe. Figure 6 reveals that below this value pronounced deviations from the expected data collapse occur, so in this regime 3D-xy scaling fails because 3D fluctuations no longer dominate. Nevertheless, at much lower fields the limit $H_c|t|^{-4/3} \propto z \to 0$ should be attainable, leading to the asymptotic behavior indicated by the solid line [Eq. (25)] in Fig. 6.

Noting again that the occurrence of 3D behavior requires that the c-axis correlation length $\xi_c=\xi_{c0}^{\pm}|t|^{-2/3}$ exceeds the interlayer spacing d it is clear that the 3D- to 2D-xy crossover is not restricted to temperatures below T_c. Given the universal ratio $\xi_{c0}^{+} \simeq \xi_{c0}^{-}/2.21$ [Eq. (4)] it even follows that above T_c the 3D-xy critical regime is even much narrower. Considering then the limits $H_c|t|^{-4/3} \propto z \to 0$ and $z \to \infty$ above T_c, Eqs. (1), (9), and (10) yield the scaling forms

$$|t|^{-2/3}\frac{m}{T} = -\frac{Q^+ c_0^+ k_B (\xi_{ab0}^-)^2}{\Phi_0^2 \xi_{c0}^-} H_c|t|^{-4/3}, \quad z \to 0 \qquad (28)$$

and

$$|t|^{-2/3}\frac{m}{T} = -\frac{Q^+ c_\infty^+ k_B \xi_{ab0}^+}{\Phi_0^{3/2} \xi_{c0}^+} (H_c|t|^{-4/3})^{1/2}, \quad z \to \infty. \qquad (29)$$

In Fig. 7 we depicted $-|t|^{-2/3}M/T$ vs $H_c|t|^{-4/3}$ for $T>T_c$ at various applied magnetic fields. The solid line is Eq. (28) in terms of

$$-|t|^{-2/3}M/T = 2\times10^{-13} H_c|t|^{-4/3}\ (\mathrm{emuK^{-1}}) \qquad (30)$$

and the dashed one

$$-|t|^{-2/3}M/T = 2.3\times10^{-9} (H_c|t|^{-4/3})^{1/2}\ (\mathrm{emuK^{-1}}), \qquad (31)$$

corresponding to the limit [Eq. (29)]. Note that Eqs. (26) and (31) fully agree with each other and with that confirm $Q^+c_\infty^+ = Q^-c_\infty^-$ [Eq. (10)]. In analogy to Fig. 6 we observe that the $z \to \infty$ limiting behavior is well confirmed, while substantial deviations from a data collapse on a single curve set in for $H_c|t|^{-4/3} \lesssim 2\times10^6$ Oe. Here the crossover to 2D-xy behavior sets in and 3D-xy scaling fails. Nevertheless, in the limit $H_c \to 0$ and reduced temperatures t in the range where 3D-xy fluctuations dominate, the limit $H_c|t|^{-4/3} \propto z \to 0$ should be attainable. It is indicated by the solid line [Eq. (30)] in Fig. 7.

According to Eq. (1) one expects that the data plotted as $M/(TH_c^{1/2})$ vs $|t|H_c^{-3/4}$ should fall on two branches. An upper branch corresponding to $T>T_c$ and a lower one for $T<T_c$. A glance at Fig. 8, depicting this plot clearly reveals the flow to 3D-xy critical behavior by approaching T_c ($|t|=0$) and in particular consistency with the leading 3D-xy critical behavior below $|t|H_c^{-3/4}=10^{-5}$ $\mathrm{Oe}^{-3/4}$.

Another property where KT behavior in terms of the 2D- to 3D-xy crossover should be observable is the magnetic field dependence of the specific peak. Indeed, in $Bi_2Sr_2CaCu_2O_{8+\delta}$ this peak shifts[18] opposite to the generic behavior.[4,6] Given the Maxwell relation,

$$\left.\frac{\partial^2 M}{\partial T^2}\right|_{H_c} = \frac{\partial}{\partial H_c}(C/T)|_T, \qquad (32)$$

relating magnetization and specific heat, this abnormality should also be observable in $\partial^2 M/\partial^2 T|_{H_c}$. A glance at Fig. 9 depicting $\partial^2 M/\partial T^2|_{H_c}$ vs T for various magnetic fields reveals consistency with the anomalous shift in the specific-heat peak. Indeed the dip shifts toward higher temperatures.

Noting that the anomalous shift occurs slightly above $T_{KT} \simeq 89.5$ K, it is indeed expected to reflect 2D-xy behavior. To check this conjecture we invoke expression (17) for

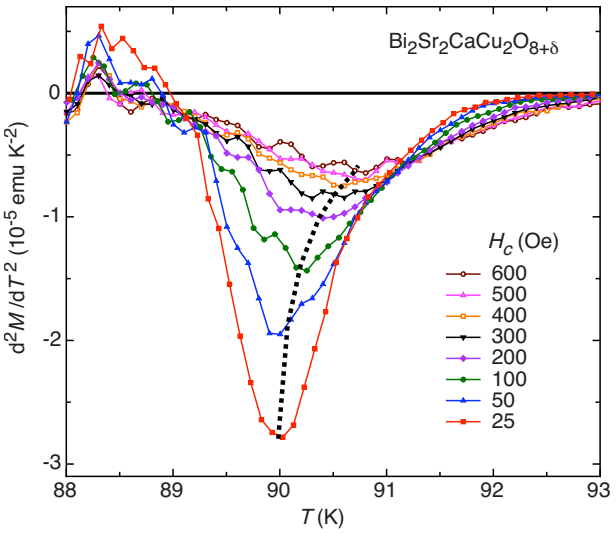

FIG. 9. (Color online) $\partial^2 M/\partial T^2|_{H_c}$ vs T at various H_c according to Eq. (32). The dotted line indicates the locations of the respective minima $T_p(H_c)$.

the magnetization valid above T_{KT} in the limit $H_c \to 0$. Although this limit is not attained in the field range considered here, m is expected to scale as $m \simeq -[k_B T/(2d\Phi_0^2)]\xi_{ab}^2 f(H_c)$ with $f(H_c)=H_c$ for $H_c \to 0$.[32] Accordingly, $\partial^2 M/\partial T^2|_{H_c}$ diverges at T_{KT}. However, there is the magnetic field induced finite-size effect preventing the correlation length ξ_{ab} to grow beyond the limiting magnetic length $L_{H_c}=[\Phi_0/(aH_c)]^{1/2}$ where $a \simeq 3.12$.[3–6] As a consequence, in finite fields the divergence is removed by a dip. Its minimum occurs at T_p given by

$$\xi_{ab}(T_p) = L_{H_c} = [\Phi_0/(aH_c)]^{1/2}. \tag{33}$$

In Fig. 10 we show T_p vs H derived from the data depicted in Fig. 9. For comparison we included

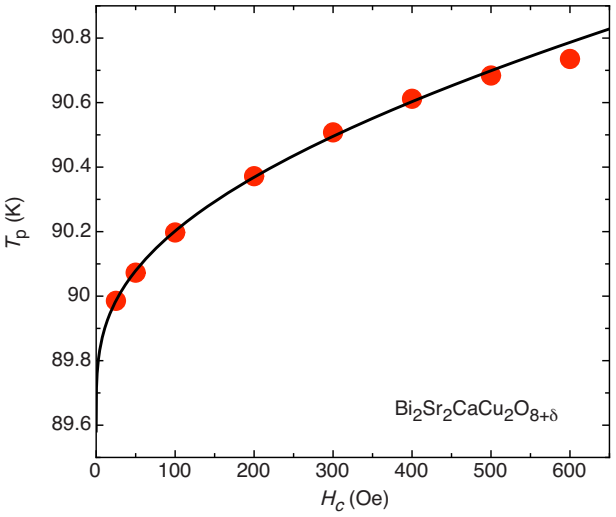

FIG. 10. (Color online) T_p vs H_c determined from the data depicted in Fig. 9. The solid line is Eq. (34) with $T_{KT}=89.5$ K, $\tilde{b} \simeq 0.3$, $a=3.12$, and $\xi_{ab0}=84$ Å.

$$T_p(H_c) = T_{KT}\left\{1 + \left[2\tilde{b}/\ln\left(\frac{\Phi_0}{a\xi_{ab0}^2 H_c}\right)\right]^2\right\}, \tag{34}$$

resulting from Eqs. (17) and (33), for a realistic set of parameters. Apparently, the characteristic shift toward higher temperatures and the $\ln(H_c)$ behavior are well confirmed and the values for $\tilde{b}$ [Eq. (17)] and $\hat{b}$ [Eq. (14)] are reasonably consistent with the relation $\tilde{b}\hat{b}=\pi/(2T_{KT}^{1/2}) \simeq 0.17$ K$^{-1/2}$ [Eq. (18)]. Furthermore, the observed H_c dependence of T_p down to 25 Oe also implies that the lateral extent L_{ab} of the homogenous regions exceeds $L_{H_c} \simeq 3640$ Å. Indeed, in the opposite case ($L_{ab} < L_{H_c}$) T_p would be independent of H_c. Thus, $L_{ab} > 3640$ Å uncovers a remarkable sample homogeneity. Nevertheless it appears to be unlikely that the asymptotic $H_c \to 0$ is experimentally attainable. Here $T_p(H_c)$ follows from $\xi_{ab}=\xi_{ab0}|T_p|^{-2/3}=L_{H_c}$ so

$$T_p = T_c\left[1 - \left(\frac{aH_c(\xi_{ab0})^2}{\Phi_0}\right)^{3/4}\right], \tag{35}$$

whereupon T_p shifts with increasing field to lower temperatures, as observed in a variety of less anisotropic cuprates.[4,6]

V. SUMMARY AND DISCUSSION

Even though the mechanism of superconductivity in the cuprates remains a mystery the associated phase-transition properties can be understood as consequences of thermal fluctuations within the framework of the theory of critical phenomena. In this work we presented and analyzed reversible magnetization data of the highly anisotropic $Bi_2Sr_2CaCu_2O_{8+\delta}$ for magnetic fields applied along the c axis of the high-quality single crystal. We examined the occurrence of 3D-xy critical behavior close to the bulk-transition temperature T_c and of Kosterlitz-Thouless behavior. Below T_c and above the presumed Kosterlitz-Thouless transition temperature T_{KT} we observed, in agreement with the theoretical prediction,[12] a downward shift in the "crossing point" toward T_{KT} from above as the field is decreased. Sufficiently below T_{KT} we verified the characteristic 2D-xy relationship between the magnetization and the in-plane magnetic penetration depth.[12] In contrast, we have seen that the measured temperature dependence of the superfluid density does not exhibit the characteristic KT behavior (Nelson-Kosterlitz jump) around the presumed T_{KT}. The absence of this feature was traced back to the 2D- to 3D-xy crossover setting in around and above T_{KT}. Indeed, in the limit $H_c|t|^{-4/3} \to \infty$ we established clear evidence for 3D-xy critical behavior above and below T_c, while in the opposite limit ($H_c|t|^{-4/3} \to 0$) its failure was attributed to the dimensional crossover. Invoking the Maxwell relation $\partial^2 M/\partial^2 T|_H = \partial(C/T)/\partial H_c|_T$ the anomalous field dependence of the specific-heat peak was also traced back to the intermediate 2D-xy behavior.[18] Implications include: first, sufficiently below T_{KT} the isotope and pressure effects on $dm/d\ln(H_c)$ at fixed temperature T and the in-plane magnetic penetration depth $\lambda_{ab}(T)$ are not independent but related by Eq. (15). Second, the bulk-transition

temperature T_c and the critical amplitudes of the c-axis correlation length and in-plane magnetic penetration depth are related by the universal relation [Eq. (8)], so the isotope and pressure effects on these properties are related.[33]

ACKNOWLEDGMENTS

This work was partially supported by the Swiss National Science Foundation and the EU Project CoMePhS.

*wstephen@physik.uzh.ch

[1] G. Blatter, M. V. Feigel'man, V. B. Geshkenbein, A. I. Larkin, and V. M. Vinokur, Rev. Mod. Phys. **66**, 1125 (1994).
[2] T. Schneider and J. M. Singer, *Phase Transition Approach to High Temperature Superconductivity* (Imperial College Press, London, 2000).
[3] T. Schneider, in *The Physics of Superconductors*, edited by K. Bennemann and J. B. Ketterson (Springer, Berlin, 2004), p. 111.
[4] T. Schneider, J. Phys.: Condens. Matter **20**, 423201 (2008).
[5] S. Weyeneth, T. Schneider, N. D. Zhigadlo, J. Karpinski, and H. Keller, J. Phys.: Condens. Matter **20**, 135208 (2008).
[6] S. Weyeneth, T. Schneider, Z. Bukowski, J. Karpinski, and H. Keller, J. Phys.: Condens. Matter **20**, 345210 (2008).
[7] T. Schneider, Physica B **326**, 289 (2003).
[8] J. M. Kosterlitz, J. Phys. C **7**, 1046 (1974).
[9] L. N. Bulaevskii, M. Ledvij, and V. G. Kogan, Phys. Rev. Lett. **68**, 3773 (1992).
[10] J. Mosqueira, L. Cabo, and F. Vidal, Phys. Rev. B **76**, 064521 (2007).
[11] J. Mosqueira and F. Vidal, Phys. Rev. B **77**, 052507 (2008).
[12] V. Oganesyan, D. A. Huse, and S. L. Sondhi, Phys. Rev. B **73**, 094503 (2006).
[13] L. Li, Y. Wang, M. J. Naughton, S. Ono, Y. Ando, and N. P. Ong, Europhys. Lett. **72**, 451 (2005).
[14] T. Jacobs, S. Sridhar, Q. Li, G. D. Gu, and N. Koshizuka, Phys. Rev. Lett. **75**, 4516 (1995).
[15] Shih-Fu Lee, D. C. Morgan, R. J. Ormeno, D. Broun, R. A. Doyle, J. R. Waldram, and K. Kadowaki, Phys. Rev. Lett. **77**, 735 (1996).
[16] K. D. Osborn, D. J. Van Harlingen, Vivek Aji, N. Goldenfeld, S. Oh, and J. N. Eckstein, Phys. Rev. B **68**, 144516 (2003).
[17] T. Schneider and D. Di Castro, Phys. Rev. B **69**, 024502 (2004).
[18] A. Junod, A. Erb, and C. Renner, Physica C **317-318**, 333 (1999).
[19] J. Hofer, T. Schneider, J. M. Singer, M. Willemin, H. Keller, C. Rossel, and J. Karpinski, Phys. Rev. B **60**, 1332 (1999).
[20] R. E. Prange, Phys. Rev. B **1**, 2349 (1970).
[21] A. Pelissetto and E. Vicari, Phys. Rep. **368**, 549 (2002).
[22] S. Watauchi, H. Ikuta, H. Kobayashi, J. Shimoyama, and K. Kishio, Phys. Rev. B **64**, 064520 (2001).
[23] D. R. Nelson and J. M. Kosterlitz, Phys. Rev. Lett. **39**, 1201 (1977).
[24] V. Ambegaokar, B. I. Halperin, D. R. Nelson, and E. D. Siggia, Phys. Rev. B **21**, 1806 (1980).
[25] A. Revcolevschi and J. Jegoudez, Prog. Mater. Sci. **42**, 321 (1997).
[26] A. Piriou, Y. Fasano, E. Giannini, and O. Fischer, Phys. Rev. B **77**, 184508 (2008).
[27] G. Triscone, A. Junod, and R. E. Gladyshevskii, Physica C **264**, 233 (1996).
[28] G. Triscone, M. S. Chae, M. C. de Andrade, and M. B. Maple, Physica C **290**, 188 (1997).
[29] H. Iwasaki, F. Matsuoka, and K. Tanigawa, Phys. Rev. B **59**, 14624 (1999).
[30] T. Schneider, Phys. Rev. B **75**, 174517 (2007).
[31] B. I. Halperin and D. R. Nelson, J. Low Temp. Phys. **36**, 599 (1979).
[32] T. Schneider, EPL **79**, 57005 (2007).
[33] T. Schneider, Phys. Rev. B **67**, 134514 (2003).